

# Methodology to Predict the Initiation of Multiple Transverse Fractures from Horizontal Wellbores

D.G. CROSBY, Z. YANG, S.S. RAHMAN  
University of New South Wales

## Abstract

Multi-stage, transversely fractured horizontal wellbores have the potential to greatly increase production from low permeability formations. Such completions are, however, susceptible to problems associated with near-wellbore tortuosity, particularly multiple fracturing from the same perforated interval. A criterion, based on that by Drucker and Prager, has been derived, which predicts the wellbore pressures required to initiate secondary multiple transverse hydraulic fractures in close proximity to primary fractures. Secondary fracture initiation pressures predicted by this new criterion compare reasonably well with those measured during a series of unique laboratory-scale multiple hydraulic fracture interaction tests. Both the multiple fracture initiation criterion and the laboratory results suggest that close proximity of primary hydraulic fractures increases the initiation pressures of secondary multiple fractures by the order of only 14%. This demonstrates that transversely fractured horizontal wellbores have limited capacities to resist the initiation of multiple fractures from adjacent perforations or intersecting heterogeneities. Petroleum engineers can use the multiple fracture initiation criterion when designing hydraulic fracture treatments to establish injection pressure limits, above which additional multiple fractures will initiate and propagate from the wellbore.

## Introduction

A significant proportion of the worldwide recoverable hydrocarbon resource exists in reservoirs possessing permeabilities of less than one milli-Darcy (mD). At present, low production rates accompanying such poor permeabilities imply that, if hydrocarbons are to be exploited economically, some form of permeability enhancement or stimulation must be carried out within these reservoirs. Even where initial permeabilities are relatively high, stimulation may still be required to overcome problems associated with localised permeability damage due to, for example, drilling mud invasion. Matrix acidisation and hydraulic fracturing remain the principal reservoir stimulation techniques.

The advantages of horizontal wells in comparison with vertical wells have been extensively documented. Indeed, in an increasing number of fields throughout the world, the production of hydrocarbons is performed exclusively through horizontal wells. Whilst still a relatively rare form of completion, fractured horizontal wells are becoming more common in low permeability formations. This is particularly so where surface geographies dictate that wells must deviate from central drill pads, such as in offshore

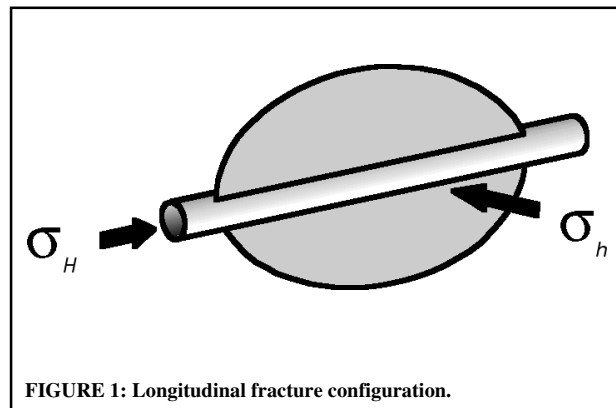


FIGURE 1: Longitudinal fracture configuration.

or arctic regions.

Hydraulic fractures, regardless of their origin, always attempt to propagate in planes orthogonal to the minimum horizontal stress, in what is commonly referred to as the “preferred fracture plane.” However, while hydraulic fracture propagation planes are fixed, the horizontal wellbores from which they emanate may assume completely arbitrary orientations. Two limiting wellbore-fracture configurations are the focus of much attention:

- “Longitudinal Fractures” propagate in planes parallel with wellbore axes, as illustrated in Figure 1. They form where horizontal wells are drilled parallel with the larger of the horizontal stresses (or parallel with the preferred fracture plane);
- “Transverse Fractures” propagate in planes orthogonal to wellbore axes, as illustrated in Figure 2. They form where horizontal wells are drilled perpendicular to the larger of the horizontal stresses (or perpendicular to the preferred fracture plane).

A number of studies have been carried out, comparing the production characteristics between fractured horizontal wells and fractured or unfractured vertical wells<sup>(1-5)</sup>. In homogeneous reservoirs, longitudinally fractured horizontal wells offer no appreciable productive advantage over similarly fractured vertical wells. Only in thin, high permeability formations will longitudinally fractured horizontal wells significantly outperform fractured vertical wells<sup>(1)</sup>.

Alternatively, transversely fractured wells have the ability to greatly increase production rates by virtue of the fact that any number of fractures may be widely distributed along the length of horizontal wells, as illustrated in Figure 2, through multi-stage treatments. The reduced contact areas between horizontal well-

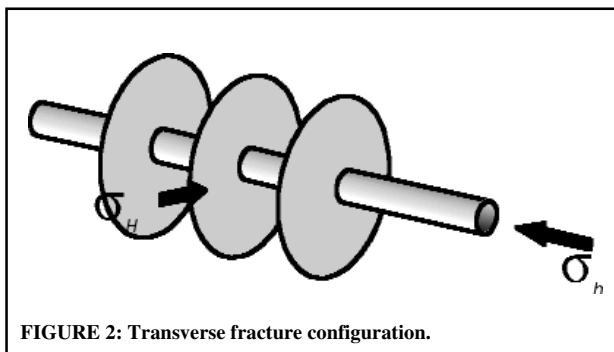


FIGURE 2: Transverse fracture configuration.

bores and transverse fractures introduce additional “choke skin effects<sup>(2)</sup>,” which hinders productivity and increases injection pressures. In general, at least three transverse hydraulic fractures are required to outproduce a single vertical well stimulated with similar dimensioned hydraulic fractures<sup>(6, 7)</sup>.

Unfortunately, transversely fractured horizontal wellbores are still plagued by a number of problems, most of which stem from the complex fracture geometries connecting the wellbore to the main fracture. These complex fracture geometries usually take the form of multiple fractures, twisted fractures, H- or S-shaped fractures<sup>(8, 9)</sup>.

The above complex fracture geometries are more commonly collectively known as “near wellbore tortuosity,” and result in narrower than anticipated fracture widths. Near-wellbore tortuosity ultimately leads to unacceptably high fracture treatment pressures, proppant bridging and pre-mature near-wellbore screenout, shorter than expected final fracture lengths, and poor fracture conductivities. The origin of these fracture complexities may be traced back to the manner in which hydraulic fractures initiate from the wellbore. A considerable amount of research is currently devoted to understanding the dynamics of hydraulic fracture initiation. Indeed, many recently adopted field practices, such as wellbore break-down using highly viscous fluids<sup>(10)</sup>, and decreased perforation densities<sup>(11)</sup>, minimise fracture tortuosity by controlling the fracture initiation process.

A number of researchers<sup>(11-14)</sup>, have suggested that every formation possesses an inherent “critical” or “threshold” fracture fluid injection pressure, above which secondary (or “auxiliary”) hydraulic fractures may initiate from natural fractures intersecting the main hydraulic fracture or wellbore. Formations with low threshold pressures may be susceptible to severe multiple fracturing and short overall hydraulic fracture lengths.

The presence of such threshold pressures can be recognised as the flat sections on log-log plots of injection pressure vs. time. Nolte and Smith<sup>(12)</sup> suggested that flaws such as natural fractures behave as “pressure regulators,” which dilate and increase fracture fluid leak-off as fluid injection pressures approach threshold pressures. In addition, both Nolte & Smith<sup>(12)</sup> and Warpinski<sup>(14)</sup> derived criteria determining the conditions required to dilate natural fractures intersecting main hydraulic fractures. Wells which have been hydraulically fractured in formations in the Wattenberg field of the Denver Basin in the United States display symptoms of natural fracture dilation with increasing fluid injection pressures<sup>(14)</sup>.

As a contribution to the above theories, this paper presents the results of analytical work carried out in order to establish the horizontal wellbore fluid pressures required to initiate additional, closely-spaced transverse multiple fractures from horizontal wellbores. In addition, the results of a series of unique laboratory multiple fracture initiation tests are presented that provide support for the analytical work.

## Theoretical Considerations

The stress state at the wall (in the direction of  $\sigma_L$ ) of a pressurised wellbore may be described in cylindrical coordinates by the following expressions:

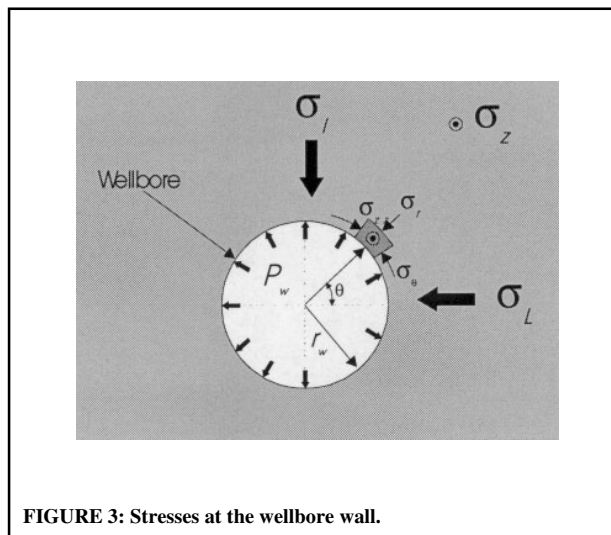


FIGURE 3: Stresses at the wellbore wall.

$$\sigma_r = P_w \quad (1)$$

$$\sigma_\theta = 3\sigma_L - \sigma_I - P_w \quad (2)$$

$$\sigma_{zz} = \sigma_z - 2\nu(\sigma_L - \sigma_I) \quad (3)$$

where:

- $\sigma_r$  = radial stress;
- $\sigma_\theta$  = tangential stress;
- $\sigma_{zz}$  = wellbore axial stress;
- $\sigma_L$  = larger in situ stress acting orthogonal to the axis of an arbitrarily oriented wellbore;
- $\sigma_I$  = smaller in situ stress acting orthogonal to the axis of an arbitrarily oriented wellbore;
- $\sigma_z$  = in situ stress acting along the axis of an arbitrarily oriented wellbore;
- $P_w$  = wellbore fluid pressure;
- $\nu$  = Poisson's ratio.

Compressive stresses are taken as positive. Figure 3 shows the orientation of the stresses described in Equations (1) to (3) on the wellbore wall. The classic Hubbert and Willis<sup>(15)</sup> expression, which makes use of Equation (2), has historically been used to estimate the wellbore fluid pressures required to initiate tensile hydraulic fractures from vertical wellbores:

$$P_{wp}^i \geq 3\sigma_h - \sigma_H + \sigma_t \quad (4)$$

where:

- $\sigma_H$  = maximum in situ horizontal stress;
- $\sigma_h$  = minimum in situ horizontal stress;
- $\sigma_t$  = rock tensile strength; and
- $P_{wp}^i$  = wellbore fluid pressure required to initiate a single (primary) fracture.

This expression assumes that fractures form when the tangential stress on the wellbore wall exceeds the rock tensile strength, and ignores the influence of pore pressure. Haimson and Fairhurst<sup>(16)</sup> derived a similar expression which accounted for poroelastic effects.

Under the stress conditions usually prevailing at the wellbore wall during fracture initiation, the tangential and radial (equivalent to wellbore fluid pressure) stresses generally assume the roles of minor and major principal stresses respectively:

$$\sigma_r > \sigma_{zz} > \sigma_\theta \quad (5)$$

That is, the wellbore axial stress ( $\sigma_{zz}$ ) is the intermediate principal stress. The classic Hubbert and Willis expression [Equation

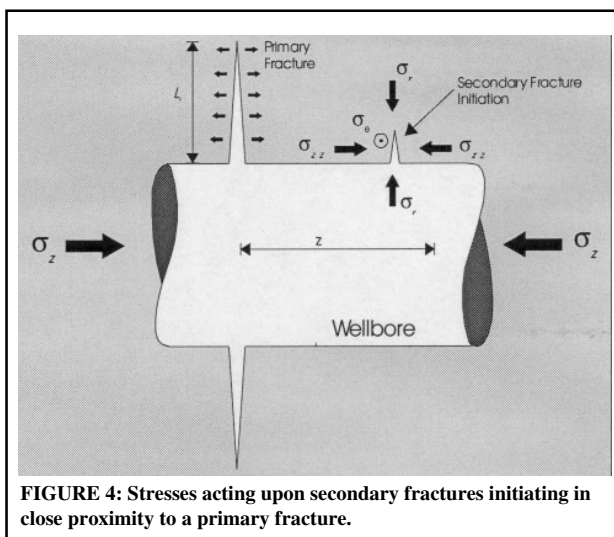


**FIGURE 4: Stresses acting upon secondary fractures initiating in close proximity to a primary fracture.**

(4)] ignores the influence of the intermediate principal stress.

However, where secondary fractures are forced to initiate in the presence of a primary fracture (illustrated in Figure 4), the wellbore axial stress (intermediate principal stress) must play some role. Therefore, any criteria estimating the conditions leading to the initiation of closely-spaced secondary fractures must incorporate intermediate principal stresses.

The influence of the intermediate principal stress on rock failure has been the subject of debate for a number of years. Experimental work carried out to establish the role of intermediate principal stresses on material failure requires relatively complex poly-axial test apparatus of the type used by Mogi<sup>(17)</sup>. As the influence of the intermediate principal stress is expected to be subtle, highly accurate load measurement is required. This is in contrast with the more widely used and simpler tri-axial tests, in which the intermediate and minor principal stresses are assumed to be equal. In addition, the highly anisotropic nature of rock compounds the difficulties associated with understanding the role of intermediate principal stresses on rock failure. Despite the difficulties, experimental work, such as that performed by Mogi, suggests that increasing intermediate principal stresses (while maintaining constant minor principal stresses) increases the magnitudes of major principal stresses at failure. Mogi also demonstrated that the degree to which the intermediate principal stress influences rock failure is closely linked to lithology.

The Drucker and Prager<sup>(18)</sup> failure criterion (often referred to as the “Extended von Mises criterion”), which accommodates the influence of the intermediate principal stress, may be used as the basis of a secondary fracture initiation criterion. The Drucker and Prager failure criterion may be simply defined by the following expression:

$$\tau_{oct} = \tau_o + \psi \sigma_{oct} \quad (6)$$

where:

$\tau_{oct}$  = “octahedral shear stress”

$$= \frac{1}{3} \sqrt{(\sigma_1 - \sigma_2)^2 + (\sigma_2 - \sigma_3)^2 + (\sigma_3 - \sigma_1)^2} \quad (7)$$

$\sigma_{oct}$  = “octahedral normal stress” (or “mean stress term”)

$$= \frac{1}{3} (\sigma_1 + \sigma_2 + \sigma_3) \quad (8)$$

$\tau_o$  and  $\psi$  are material properties which must be determined experimentally.  $\sigma_1$ ,  $\sigma_2$  and  $\sigma_3$  are the major, intermediate and minor principal stresses, respectively. This criterion is widely used as a means of assessing wellbore stability<sup>(19, 20)</sup>.

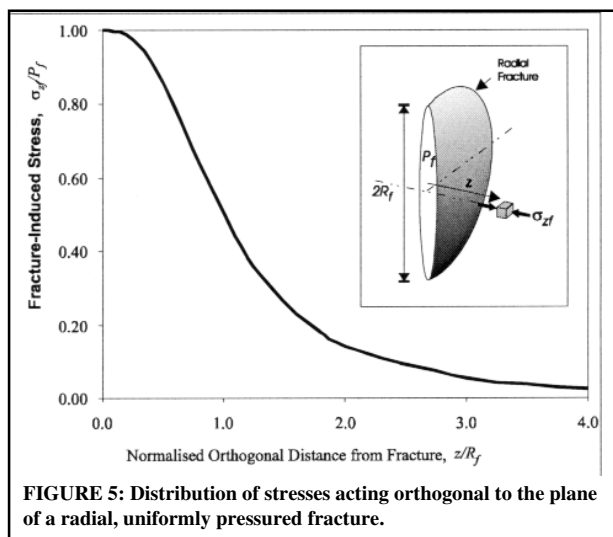


**FIGURE 5: Distribution of stresses acting orthogonal to the plane of a radial, uniformly pressured fracture.**

As described previously by Equation (5), the radial ( $\sigma_r$ ), axial ( $\sigma_{zz}$ ) and tangential stresses ( $\sigma_\theta$ ) at wellbore walls assume the roles of major, intermediate and minor principal stresses, respectively, at depths typically of interest to the petroleum industry. Recall that, at the wellbore wall, radial stress is equivalent to wellbore fluid pressure. Therefore, in terms of the stresses acting on wellbore walls at failure, octahedral shear and normal stresses may be defined as follows:

$$\tau_{oct} = \frac{1}{3} \sqrt{(P_{wp}^i - \sigma_{zz})^2 + (\sigma_{zz} - \sigma_\theta)^2 + (\sigma_\theta - P_{wp}^i)^2} \quad (9)$$

$$\sigma_{oct} = \frac{1}{3} (P_{wp}^i + \sigma_{zz} + \sigma_\theta) \quad (10)$$

where  $P_{wp}^i$  is the wellbore fluid pressure required to initiate a single (primary) fracture. In addition, where the wellbore is oriented in a principal in situ stress direction, the tangential stress may be expressed in terms of the in situ stresses acting orthogonal to the wellbore axis, and the wellbore fluid pressure:

$$\sigma_\theta = 3\sigma_l - \sigma_L - P_{wp}^i \quad (11)$$

By substituting Equations (9), (10) and (11) into the Drucker and Prager expression [Equation (6)], the following modified expression is derived:

$$\frac{1}{3} \sqrt{(P_{wp}^i - \sigma_{zz})^2 + (\sigma_{zz} - 3\sigma_l + \sigma_L + P_{wp}^i)^2 + (3\sigma_l - \sigma_L - 2P_{wp}^i)^2} = \tau_o + \frac{\psi}{3} (3\sigma_l - \sigma_L + \sigma_{zz}) \quad (12)$$

The above expression may be solved for  $P_{wp}^i$ .

The wellbore axial stress ( $\sigma_{zz}$ ) is a function of primary fracture proximity (2s) and pressure ( $P_{fp}$ ). The local stresses exerted by radial fractures may be described analytically, such as by solutions derived by Sneddon<sup>(21)</sup>, which is illustrated graphically in Figure 5. This figure demonstrates that localised stress increases induced by hydraulic fractures diminish rapidly with increasing distance away from the fractures. Therefore, unless secondary fractures initiate within close proximity to a primary fracture, the wellbore pressures required to initiate secondary fractures will be no greater than those required to initiate single, isolated hydraulic fractures. However, in many cases, particularly where the pressurised intervals in horizontal wells are small, or during the hydraulic fracturing of vertical wells, secondary hydraulic frac-

**TABLE 1: Summary of the laboratory-scale fracture test parameter, and comparisons with field dimensions.**

Parameter	Field-Scale Dimension	Lab.-Scale Dimension
<i>Wellbore Dimensions:</i>		
Wellbore radius, $r_w$ (m)	0.091	0.006
<i>Reservoir Properties:</i>		
Permeability, $K$ (mD)	0.1	8e-5
<i>Geomechanical Properties:</i>		
Elastic modulus, $E$ (MPa)	50,000	700
Poisson's ratio, $\nu$	0.25	0.2
Fracture toughness, $K_{IC}$ ( $MPa\sqrt{m}$ )	3	0.27
<i>Laboratory-Derived Drucker &amp; Prager Parameters:</i>		
$\tau_o$		7.72
$\Psi$		0.73
<i>In situ Stresses:</i>		
Vertical in situ stress, $\sigma_v$ (MPa)	64	7
Min. in situ horiz. Stress, $\sigma_h$ (MPa)	47	5
Max. in situ horiz. Stress, $\sigma_H$ (MPa)	57	6
<i>Hydraulic Fracture Treatment Data:</i>		
Leak-off, $k_l$ ( $m/\sqrt{s}$ )	4.8e-5	3.8e-8
Injection rate, $Q$ (m <sup>3</sup> /s)	0.072	3e-7 - 1e-6
Injection period, $t$ (min)	27	1
Fracture fluid viscosity, $m$ (Pa s)	0.5	30 (@ 23° C)

tures may indeed be forced to initiate in close proximity to primary fractures. In addition, primary fractures initiated from wells in formations unbounded by more highly stressed intervals may grow to significant radii prior to secondary fracture initiation.

Where secondary fractures initiate close to a primary fracture, the wellbore axial stress ( $\sigma_{zz}$ ), against which the secondary fracture must form, approaches that of the primary fracture pressure. Under such 'zero-spaced' conditions, the single fracture Drucker and Prager criterion described by Equation (12) can be modified such that it assumes the following form:

$$\frac{1}{3} \sqrt{(P_{ws}^i - P_{fp})^2 + (P_{fp} - 3\sigma_l + \sigma_L + P_{ws}^i)^2 + (3\sigma_l - \sigma_L - 2P_{ws}^i)^2} = \tau_o + \frac{\Psi}{3}(3\sigma_l - \sigma_L + P_{fp}) \quad (13)$$

where:

$P_{fp}$  = uniform primary fracture pressure;

$P_{ws}^i$  = wellbore pressure required to initiate secondary hydraulic fracture.

Equation (13) can then be solved for  $P_{ws}^i$ . In the field, however, individual hydraulic multiple fractures are not hydraulically isolated. This is in contrast with the 'static' multiple fracture initiation described by Equation (13). Indeed, the fluid pressures within the primary and secondary fractures are coupled. Thus the modified Drucker and Prager multiple fracture initiation criterion described by Equation (13) must be solved iteratively. The dynamic solution process simply involves substituting, at each iteration, the wellbore pressure required to initiate a secondary fracture ( $P_{ws}^i$ ), into the uniform pressure within the primary fracture ( $P_{fp}$ ). This process is repeated until convergence.

## Laboratory-Scale Fracture Studies Experimental Set-up

A series of laboratory-scale hydraulic fracture experiments have been carried out in an attempt to model the initiation and propagation of, and interaction between, multiple transverse fractures. Only the fracture initiation aspects of the experimental work will be described in this paper. The fracture propagation issues will be discussed in future publications.

In order to produce representative results, the laboratory tests adhered to the strict scaling procedures outlined by de Pater et al.<sup>(22)</sup> The laboratory test dimensions were scaled upon those typically encountered during the exploitation of low permeability gas resources in Central Australia. Length dimensions were scaled according to wellbore radius ( $r_w$ ). Extremely low injection rates were employed in order to achieve stable fracture initiation and growth. This necessitated the use of an extremely high viscosity fracture fluid and a low leak-off fracture medium. Correct scaling also required that the fracture medium possess a low modulus ( $E$ ) and toughness ( $K_{IC}$ ).

A high viscosity (30 Pa•s at 23° C) industrial lubricant was employed as a fracture fluid. The fracture test material was a Portland cement-based material composed of the following:

Off-white Portland cement	30%*
Silica flour	70%*
Water/cement ratio	0.35*
Acrylic emulsion/water ratio:	1:7.1*
Water Reducing Agent:	2,000 ml/100 kg Portland cement

(\* by weight of total cementitious material)

The low cement content ensured that the fracture test material possessed a low elastic modulus (7,000 MPa) and low toughness (0.27  $MPa\sqrt{m}$ ). In addition, the high proportion of silica flour and inclusion of acrylic emulsion provided the test material with a negligible permeability (8e-5 mD). Table 1 summarises laboratory test material properties, and compares them with those in the field.



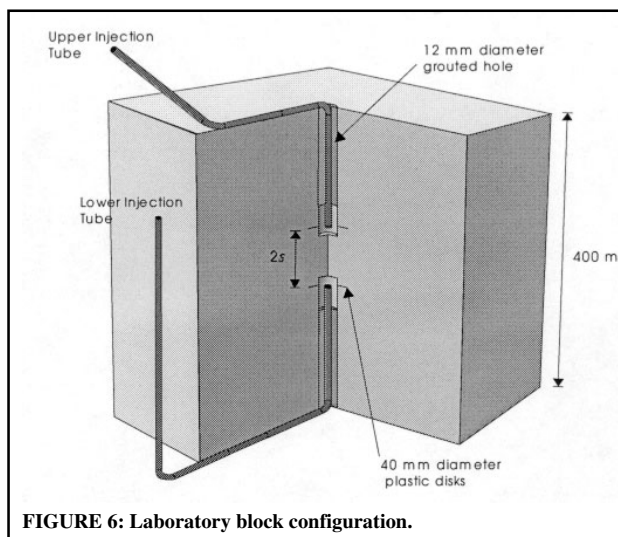


FIGURE 6: Laboratory block configuration.

The synthetic fracture test material was cast into blocks measuring  $400 \times 400 \times 400$  mm. Thin circular plastic disks were positioned inside the blocks during casting (Figure 6). When intersected by a wellbore, these disks constrained the location at which hydraulic fractures initiated. The disks were separated by a distance 30 mm, and were intersected by two, hydraulically isolated wellbores, each possessing a radius of 6 mm. Stainless steel injection tubes, of 3 mm internal radius, were grouted into the wellbores, leaving a small "open hole" section immediately adjacent to the plastic disks. The absence of a sand fraction left the synthetic fracture medium susceptible to shrinkage cracking. However, this was minimised by storing the blocks under conditions of 100% humidity during curing, and until immediately prior to testing.

The blocks were placed in a poly-axial cell, as illustrated in Figure 7. Through the use of water-filled flat-jacks, the poly-axial cell exerted stresses on all faces of each block. The magnitudes of the applied stresses (Table 1) were such that the wellbores were oriented in the direction of the minor principal stress. This orientation between wellbore and stresses promoted the formation of transverse hydraulic fractures. Two computer-controlled linear displacement pumps, shown in schematic form in Figure 8, were used to inject fracture fluid independently into each wellbore. In addition, transducers independently measured the initiation and propagation pressures of each multiple fracture. The injection

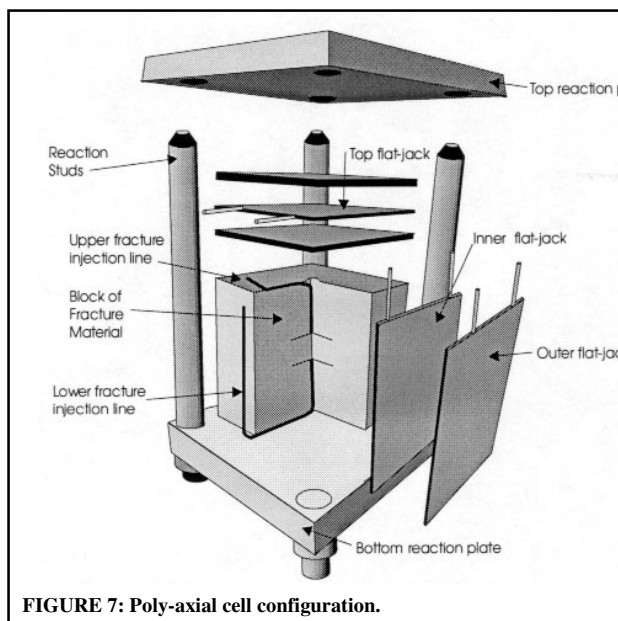


FIGURE 7: Poly-axial cell configuration.

pressure record for multiple fracture Test #3 is illustrated in Figure 9. The fracture pressures displayed in Figure 9 have been corrected for compressibility of the injection system and fracture fluid. During injection testing, both wellbores were pressurised at similar rates. A primary fracture eventually initiated from one of the two wellbores. Immediately after the primary fracture initiated, the wellbore from which it emanated was shut-in. Injection into the primary fracture recommenced only after the secondary fracture (from the opposing wellbore) was initiated. Injection into both fractures was allowed to proceed at a constant rate for a period of approximately two minutes, whereupon they were both shut-in.

## Results

The Drucker and Prager material constants ( $\tau_o$  and  $\psi$ ) were derived through tri-axial testing of the fracture test material, and are listed in Table 1. By substituting these material constants and the applied in situ stresses ( $\sigma_1$ ,  $\sigma_L$  and  $\sigma_z$ ) into Equation (13), the following criterion is derived:

$$\frac{1}{3} \sqrt{(P_{ws}^i - P_{fp})^2 + (P_{fp} - 1I + P_{ws}^i)^2 + (1I - 2P_{ws}^i)^2} = 7.72 + 0.245(P_{fp} + 1I) \quad (14)$$

This criterion can be used to estimate the wellbore fluid pressure ( $P_{ws}^i$ ) required to initiate secondary hydraulic fractures in the presence of a nearby inflated primary fracture. The laboratory fracture test provided a unique opportunity to establish the validity of this modified criterion.

As described previously, field-scale primary and secondary fracture pressures are coupled. This contrasts with the experimental configuration, in which the primary and secondary multiple fractures initiated and propagated in hydraulic isolation. However,

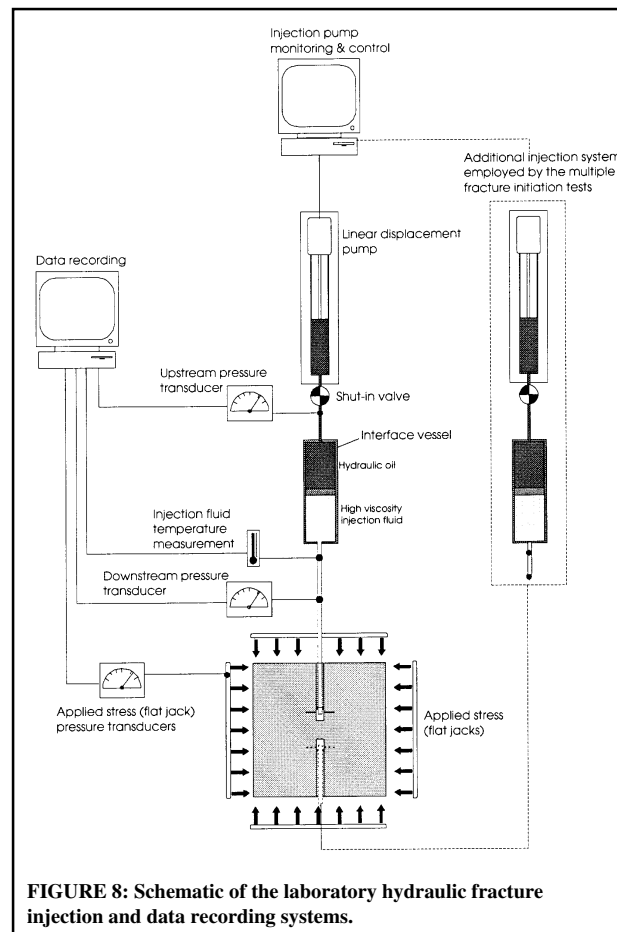


FIGURE 8: Schematic of the laboratory hydraulic fracture injection and data recording systems.

# Explore Litigation Insights

Docket Alarm provides insights to develop a more informed litigation strategy and the peace of mind of knowing you're on top of things.

## Real-Time Litigation Alerts



Keep your litigation team up-to-date with **real-time alerts** and advanced team management tools built for the enterprise, all while greatly reducing PACER spend.

Our comprehensive service means we can handle Federal, State, and Administrative courts across the country.

## Advanced Docket Research



With over 230 million records, Docket Alarm's cloud-native docket research platform finds what other services can't. Coverage includes Federal, State, plus PTAB, TTAB, ITC and NLRB decisions, all in one place.

Identify arguments that have been successful in the past with full text, pinpoint searching. Link to case law cited within any court document via Fastcase.

## Analytics At Your Fingertips



Learn what happened the last time a particular judge, opposing counsel or company faced cases similar to yours.

Advanced out-of-the-box PTAB and TTAB analytics are always at your fingertips.

## API

Docket Alarm offers a powerful API (application programming interface) to developers that want to integrate case filings into their apps.

## LAW FIRMS

Build custom dashboards for your attorneys and clients with live data direct from the court.

Automate many repetitive legal tasks like conflict checks, document management, and marketing.

## FINANCIAL INSTITUTIONS

Litigation and bankruptcy checks for companies and debtors.

## E-DISCOVERY AND LEGAL VENDORS

Sync your system to PACER to automate legal marketing.